

Unfolding Restricted Convex Caps

Joseph O’Rourke*

July 16, 2021

Abstract

This paper details an algorithm for unfolding a class of convex polyhedra, where each polyhedron in the class consists of a convex cap over a rectangular base, with several restrictions: the cap’s faces are quadrilaterals, with vertices over an underlying integer lattice, and such that the cap convexity is “radially monotone,” a type of smoothness constraint. Extensions of Cauchy’s arm lemma are used in the proof of non-overlap.

1 Introduction

Few classes of convex polyhedra are known to be *edge-unfoldable*: unfolded by cutting along edges of the polyhedron and flattening into the plane to a single piece without overlap. Among the classes known to be are: pyramids, prismoids, and “domes.” See [DO07, Chap. 22] for background on this problem.

The purpose of this informal note is to introduce another narrow class of polyhedra for which an edge-unfolding algorithm can be provided. We call this class *radially monotone lattice quadrilateral convex caps*. The long name reflects the several qualifications needed to guarantee correctness, qualifications that hopefully can be removed by subsequent research. The upper surface of such a polyhedron \mathcal{P} is a *convex cap* C in the sense that C projects parallel to the z -axis to its base B in the xy -plane without overlap. In other words, the intersection of the cap C with a line parallel to z through an interior point of B is a single point. In other terminology, C is a *terrain*. C is composed entirely of quadrilaterals, each of which projects to a unit lattice square in the xy -plane, and whose projections tile B . The base B is restricted to be a rectangle. \mathcal{P} then is the convex hull of $C \cup B$, which fills in the four sides S_{x^-} , S_{x^+} , S_{y^-} , S_{y^+} . See Figure 1(a,b). The “radially monotone” qualification restricts the “sharpness” of the convexity of the cap in a way that is not easily explained until we develop more notation.

A more general shape would be a *lattice convex cap*, the convex hull of B and a set of points (x, y, z) over each integer lattice point (x, y) in B . Here

*Dept. Comput. Sci., Smith College, Northampton, MA 01063, USA. orourke@cs.smith.edu.

the faces are in general triangles rather than quadrilaterals, and C is a *convex height field*. The restriction to quadrilaterals narrows the class considerably, as we now show.

Quadrilateral Restriction. Let the base B range over the lattice points $x = 1, \dots, n_x$ and $y = 1, \dots, n_y$. If the points above the front and left of B are specified,

$$c_x(1) : \{(x, 1) : x = 1, \dots, n_x\}$$

and

$$c_y(1) : \{(1, y) : y = 1, \dots, n_y\}$$

then all the points above the remainder of B are determined. This can be seen as follows. If three of the four corners of a lattice cell are given,

$$(x, y, z_0), (x + 1, y, z_1), (x, y + 1, z_3)$$

then the fourth corner, $(x + 1, y + 1, z_2)$, is determined by the plane containing the first three corner points, whose height can be computed as

$$z_2 = -z_0 + z_1 + z_3 \tag{1}$$

Thus,

$$(1, 1, z_0), (2, 1, z_1), (1, 2, z_3)$$

determine $(2, 2, z_2)$, and this determination propagates similarly out over the entire $n_x \times n_y$ rectangle. Thus, if $n_x = n_y = n$, the n^2 lattice points of B are fixed by specifying just the $2n - 1$ values along the front and left sides. A consequence of Lemma 2 below is that a lattice quadrilateral cap C is convex if and only if the curves at its two boundaries $c_x(1)$ and $c_y(1)$ (i.e., the upper boundaries of S_{x^-} and S_{y^-}) are convex.

Radially Monotone. The full definition of when a convex cap is radially monotone will be deferred until Section 5 below, where it is first employed. Here we define when a planar convex curve is radially monotone, and give two sufficient conditions for radial monotonicity of a convex cap. Let c be a convex curve, and let p_0 and p_i be two vertices of the curve, with p_{i+1} the vertex following p_i . Then c is *radially monotone* if the angle $\angle p_0 p_i p_{i+1} \geq \pi/2$, for every pair of vertices p_0 and p_i . The condition may be interpreted as requiring that the next segment $p_i p_{i+1}$ of the chain does not penetrate the circle of radius $|p_0 p_i|$ centered on p_0 . So points on the chain increase their radial distance from p_0 . (See ahead to Figure 5.) The two sufficient conditions are as follows:

1. If the two convex curves $c_x(1)$ and $c_y(1)$ are both radially monotone, then the convex cap is radially monotone.
2. If each of these convex curves fits in a semicircle connecting its two endpoints, then each is radially monotone, and so (1) applies.

This latter condition justifies the notion that radial monotonicity enforces a type of smoothness on the convexity of the cap.

2 Lattice Quadrilateral Cap Properties

We now derive several properties of lattice quadrilateral convex caps.

Lemma 1 (Parallelograms) *Every quadrilateral over a lattice cell is a parallelogram.*

Proof: Let the four corners of the quadrilateral be a, b, c, d in counterclockwise order, let α and β be the angles at a and b respectively, and let Π be the plane containing the quadrilateral. We argue that the two coplanar triangles $\triangle abd$ and $\triangle bcd$ are congruent. They share the diagonal of the quadrilateral, bd . The edge ab must be congruent to edge dc , because both are the intersection of Π with a unit vertical strip, parallel (say) to the xz -plane. Therefore $|ab| = |dc|$. Similarly, bc must be congruent to ad , because both are produced by Π intersecting the a unit vertical yz -strip. Therefore $|bc| = |ad|$. Therefore $\triangle abd$ and $\triangle bcd$ have all edges the same length, and so are congruent, as claimed. So the angles at a and at c are the same, α . Similarly, the angles at b and at d are the same, β . \square

Call the chain of edges of C above $(y, 1), (y, 2), \dots, (y, n_x)$ the x -chain $c_x(y)$, and similarly define the y -chain $c_y(x)$.

Lemma 2 (Cap Convexity) *For a lattice quadrilateral cap C , all the x -chains are congruent to one another, as are all the y -chains.*

Proof: Consider two consecutive edges of the x -chain $c_x(y)$, over $(x, y), (x + 1, y), (x + 2, y)$. By the Parallelogram Lemma (1), the corresponding edges in the next x -chain $c_x(y + 1)$ are parallel to those in $c_x(y)$. Thus the convex angle at the middle point $(x + 1, y)$ is exactly the same as that at $(x + 1, y + 1)$. Because this is true at every lattice point of each x -chain, all are congruent. \square
The congruency of the chains is evident in Figure 1(a,b).

Let $z(x, y)$ be the point of C above (x, y) .

Lemma 3 (Cap Maxima) *The maximum z -height of a lattice quadrilateral cap C for the points at a particular x -value, $\max_y z(x, y)$, is achieved at a y -value y_{max} independent of x . And the same claim holds when the roles of x and y are interchanged.*

Proof: This follows immediately from the congruency of the x -chains provided by Lemma 2. \square

For example, in Figure 1(a,b), $y_{max} = 14$.

3 Sketch of Algorithm

We first sketch the unfolding algorithm, using Figure 1 for illustration, before justifying it in the following sections. The strip of quadrilaterals between y_{max} and $y_{max} + 1$, call it the y_{max} -strip is unfolded with $(1, y_{max})$ at the origin and its leftmost edge along the y -axis. Thus it unfolds roughly horizontally. See the

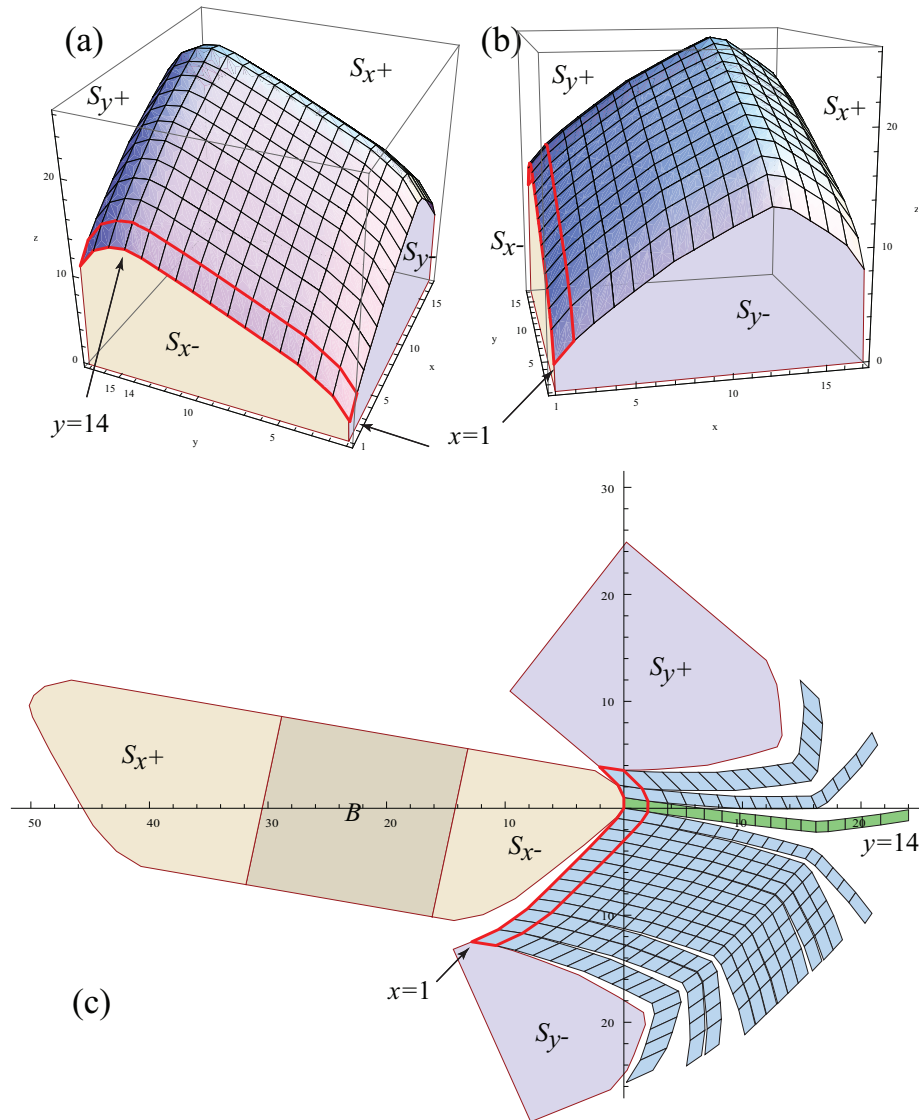


Figure 1: (a,b) Two views of the same convex cap C . The base B is the square at $z = 0$. (c) Unfolding of \mathcal{P} .

green $y = 14$ strip in Figure 1(c). All the other “parallel” x -strips for different y -values are arranged above and below this y_{max} -strip, connected along the uncut edge between $x = 1$ and $x = 2$. All other x -edges for $x \geq 2$ are cut. We will show that these strips splay outward from the y_{max} -strip, avoiding overlap. The two side faces $\{S_{x-}, S_{x+},\}$ are unfolded attached to the base B , and attached to the cap unfolding at the leftmost vertical edge of the y_{max} -strip. We will show that S_{x-} in particular does not overlap with the $x = 1, 2$ strip (outlined in red in the figure). The remaining two side faces, $\{S_{y-}, S_{y+}\}$, are attached at the two ends of the $x = 1$ strip as shown in the figure.

4 Quadrilateral Angles

We will call the four angles of a quadrilateral $(\alpha, \beta, \alpha, \beta)$ in counterclockwise order. Note that $\alpha + \beta = \pi$, so one angle determines all the others. Much of our reasoning relies on an analysis of the behavior of the quadrilateral angles.

Fix one quadrilateral over its lattice cell, with corner heights $z_0 = 0, z_1, z_2, z_3$, counterclockwise above $(0, 0), (1, 0), (1, 1), (0, 1)$ respectively, as in Figure 2(a). We will need detailed knowledge of how the $(0, 0)$ corner angle α varies as a function of z_1 and z_3 :

Lemma 4 (One Quad) *For $z_3 > 0$, $\alpha(z_1)$ is a strictly decreasing function of z_1 , passing through $\pi/2$ at $z_1 = 0$. $\alpha(z_1, -z_3) = \pi/2 - \alpha(z_1, z_3)$, so, for $z_3 < 0$, $\alpha(z_1)$ is a strictly increasing function of z_1 .*

Proof: Explicit calculation shows that

$$\alpha = \alpha(z_1, z_3) = \cos^{-1} \left(\frac{-z_1 z_3}{\sqrt{1+z_1^2} \sqrt{1+z_3^2}} \right)$$

The claimed properties follow from the properties of the inverse cosine function. See Figure 2(b). \square

We now examine angles formed by two adjacent quadrilaterals. We fix one in the position detailed above, and the other adjacent to its left, with height z'_1 above the lattice point $(-1, 0)$. Note that the other three corners of this second quadrilateral are then determined. Let θ be the angle in the vertical plane containing the edges above $(-1, 0), (0, 0), (1, 0)$, and let α and β' be the angles of the quadrilateral incident to the origin $(0, 0, 0)$. See Figure 3(a). We need the behavior of $(\alpha + \beta')$ as z_3 varies:

Lemma 5 (Two Quads) *Let the front edges of two adjacent quadrilaterals make a convex angle of θ in the vertical plane containing those edges. Then $(\alpha + \beta')$ is a strictly increasing function of z_3 , passing through π at $z_3 = 0$, and with asymptote θ for $z_3 < 0$ and $2\pi - \theta$ for $z_3 > 0$.*

Proof: A proof by explicit calculation, using the formula used in the One-Quad Lemma (4) twice, will not be presented. Alternatively, one can arrive

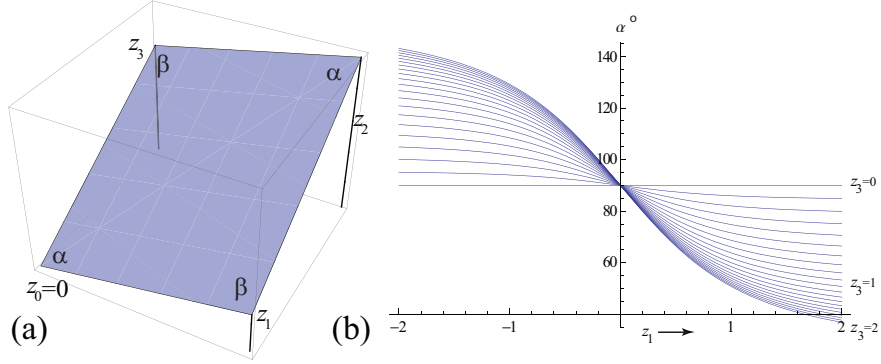


Figure 2: (a) one quadrilateral; (b) $\alpha(z_1, z_3)$ is strictly decreasing for $z_3 > 0$.

at the claim via the One-Quad Lemma as follows. From Figure 2, α decreases as z_3 increases, but, because $|z'_1| > z_1$ by convexity, β' increases more than α decreases, and so $\alpha + \beta'$ increases. See Figure 3(b) for sample plots. Note that, as $z_3 \rightarrow +\infty$, α and β' approach lying in the vertical plane above θ , and so $\theta + \alpha + \beta' = 2\pi$, and as $z_3 \rightarrow -\infty$, $\alpha + \beta' \rightarrow \theta$. \square

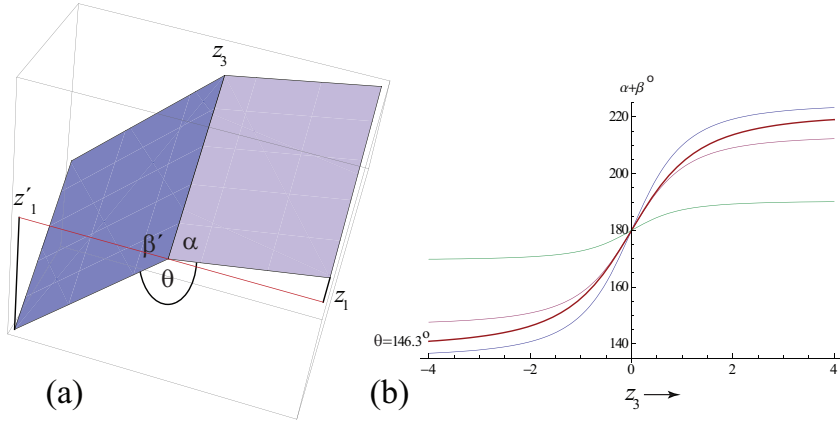


Figure 3: (a) Two adjacent quadrilaterals; here $\theta = 146.3^\circ$. (b) $(\alpha + \beta')$ is a strictly increasing function of z_3 ; Note the asymptote $\theta = 146.3^\circ$ for the highlighted curve corresponding to (a).

Define the *turn angle* τ at point of a curve with convex angle θ to be $\pi - \theta$.

Lemma 6 (Strip Unfolding) *Each strip of quadrilaterals unfolds without self-overlap, with convex boundary curves.*

Proof: Let an x -strip lie between y and $y + 1$. Let $\theta(x)$ be the angle at

$p = (x, y, z(x, y))$ in the vertical y -plane through p . We know from the Convex Cap Lemma (2) that $\theta \leq \pi$ because the curve is convex at p . Let $\tau_0 = \pi - \theta$ be the turn angle at p in the vertical plane. The turn angle of the unfolded quadrilaterals incident to p is $\tau = (\alpha + \beta') - \pi$. The Two-Quad Lemma (5) shows that $(\alpha + \beta') \in [\theta, 2\pi - \theta]$, which implies that $\tau \in [\theta - \pi, \pi - \theta]$, i.e., $\tau \in [-\tau_0, +\tau_0]$. These are precisely the angle conditions for application of the extension of Cauchy's arm lemma: all turn angles of the convex curve are "straightened" [O'R01]. (This is an extension of Cauchy's arm lemma because nonconvexities might be introduced.) The usual conclusion is that, under such a *valid reconfiguration*, the endpoints of the chain pull further apart. In [O'R03, Cor. 2] this consequence is derived: A valid reconfiguration of an open convex chain remains simple, i.e., does not self-intersect.

Although in general a valid reconfiguration could result in a nonconvex straightened curve, in our case the Convex Cap Lemma (2) places us to the left or right of $z_3 = 0$ in Figure 3(b), keeping all turn angles τ the same sign, and therefore resulting in a convex curve.

So now we have established that neither of the two unfolded boundary curves of the x -strip, call them u_y from the chain at y and u_{y+1} that at $y + 1$, self-intersect. But by the Parallelograms Lemma (1), u_y and u_{y+1} are connected by, and therefore separated by, edges that are all parallel. (See Figures 1(c), 8, and 9.) Thus u_y cannot intersect u_{y+1} . Finally, these parallel "ladder bars" ensure that it is not possible for the first x -segment to intersect the last x -segment. Therefore the entire strip unfolds without self-overlap. \square

Finally we move to an analysis of four quadrilaterals, needed to compare turn angles in the unfolding.

Lemma 7 (Four Quads) *Let four quadrilaterals be incident to the origin $o = (0, 0, 0)$, with those touching $y = 1$ the upper quads and those touching $y = -1$ the lower quads. Let the upper quads unfold with turn angle τ at o , and the lower quads with turn τ_0 at o . Then, if the middle edge of the lower quads, over $(0, -1), (0, 0)$, is uphill w.r.t. z ($z'_3 < 0$ in the notation below), then $\tau_0 \geq \tau$: the lower quads unfold to turn more sharply.*

Proof: We extend the analysis in the Two-Quad Lemma (5) to four quadrilaterals incident to a central point, taken to be $o = (0, 0, 0)$ without loss of generality. We repeat all the notation developed in that lemma and displayed in Figure 3(a), and add two new quadrilaterals, determined by one new parameter $z'_3 < 0$, as shown in Figure 4, with angle labels as indicated. Knowing from the Convex Cap Lemma (2) that the two convex x -chains are congruent, we know they determine the same θ in vertical planes, and so Lemma 5 can be applied on an equal footing to both chains. Our goal is to compare the angle $A = \alpha + \beta'$ to $B = \alpha'_0 + \beta_0$, for these angles determine the turn angles. Note that A is the same angle studied in the Two-Quads Lemma (5), but $B = 2\pi - (\alpha_0 + \beta'_0)$, where $(\alpha_0 + \beta'_0)$ is the angle to which Lemma 5 applies.

Now, in order to maintain convexity along the y -chain through the central point, we must have $|z'_3| \geq z_3$ (recall the central point is the origin, so $z'_3 < 0$).

Because $|z'_3|$ is right of z_3 in Figure 3(b), and the angle sum is strictly increasing, we know that $\alpha_0 + \beta'_0 \geq \alpha + \beta'$, i.e., $2\pi - B \geq A$. Let τ be the turn angle at o of the unfolding of the upper two quads, $\tau = A - \pi$, and τ_0 the same turn angle of the lower two quads, $\tau_0 = \pi - B$. Substitution into the inequality $2\pi - B \geq A$ yields $\tau_0 \geq \tau$. \square

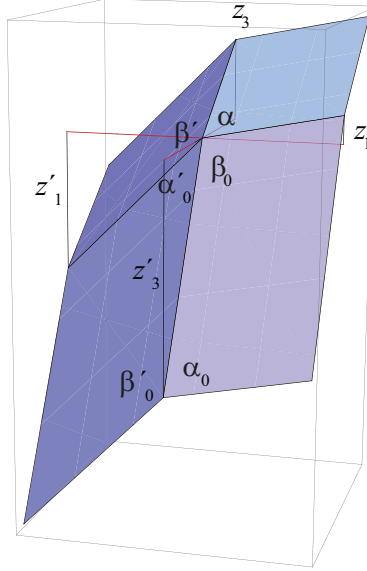


Figure 4: Four quadrilaterals incident to $(0,0,0)$. Convexity implies that $|z'_3| \geq z_3$.

The sharper turn angles guaranteed by this lemma provide a type of separation between adjacent strips, but not enough to ensure non-overlap.

5 Radial Monotonicity

Now we finally come to the point where we need to use radial monotonicity, to guarantee that the unfolding of adjacent strips do not overlap. The condition we need is that the unfolded edge of each quadrilateral strip be radially monotone, in the sense defined in Section 1 above. The Strip Unfolding Lemma (6) shows that the unfolded strip boundary is a straightening of the curve $c_x(y)$ in the vertical plane, so that radial monotonicity of $c_x(y)$ implies radial monotonicity of the strip boundary, which justifies the first sufficient condition claimed in Section 1.

We now show that any opening/straightening of a radially monotone curve avoids overlap:¹

¹ It may be that the equivalent of this lemma is available in the literature, but no explicit reference could be found.

Lemma 8 (Radial Monotonicity) *Let c' be a straightening of a convex curve c , i.e., a reconfiguration such that every convex angle either stays the same or opens closer to (but not exceeding) π . Let c lie in the positive quadrant with origin o , with the left endpoints of both c and c' at o . If c is radially monotone, then c' does not intersect c except at o .*

Proof: First consider the curve c_2 in Figure 5, which is not radially monotone at a because $\angle oab < \pi/2$. One can see that segment ab cuts into the circle of radius $|oa|$, and that under rotation about o , $a'b'$ crosses ab . On the other hand, curve c_1 in the figure is radially monotone, with each succeeding segment connecting two concentric circles. Now rotation about o moves each segment of c_1 on those circles, and thus keeps the segment confined to the annulus between. Therefore such rotation cannot intersect any part of c_1 .

Now because the lemma assumes that c lies in the positive quadrant, it is radially monotone from any other vertex p beyond o , for the angle $\angle pab$ can only be larger than $\angle oab$. Now we view the opening of c as composed of rotations about each joint playing the role of o successively. As the chain is rigid beyond each rotation pivot o , the radial monotonicity beyond o is not affected. So none of the rotations can cause overlap, and the lemma is established. \square

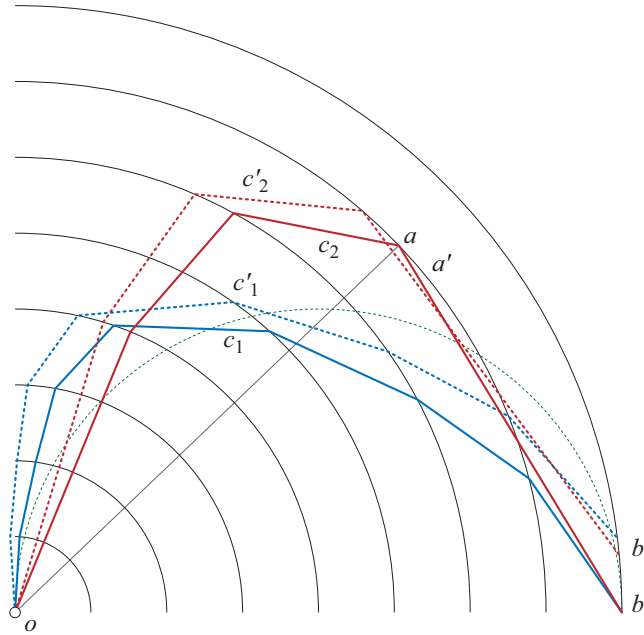


Figure 5: c_1 is radially monotone, and $c'_1 \cap c_1 = \{o\}$; c_2 is not, and $ab \cap a'b' \neq \emptyset$.

Note that if c stays inside the semicircle connecting its endpoints (drawn lightly in Figure 5), then radial monotonicity is guaranteed (because every point on the semicircle subtends $\pi/2$ from the diameter). This justifies the second suf-

sufficient condition claimed in Section 1. (None of the various sufficient conditions mentioned are necessary, e.g., c_1 in the figure does not fit in the semicircle but is nevertheless radially monotone.)

Lemma 9 (Adjacent Strips) *Adjacent x -strips of quadrilaterals unfold without overlap.*

Proof: This now follows immediately from the Four-Quad Lemma (7), which establishes that adjacent strip boundaries correspond to a convex curve c and a straightening c' (because τ_0 , corresponding to c' , is $\geq \tau$, corresponding to c), and the Radial Monotonicity Lemma (8), which guarantees non-overlap of the two curves. \square

Clearly the same reasoning guarantees the non-overlap of the side faces S_{x-}, S_{y-}, S_{y+} with their adjacent quadrilateral strips. See Figures 8 and 9 for further examples of cap unfoldings.

That the radial monotonicity restriction is sometimes necessary is established by the overlapping unfolding of a convex cap that has such a plummet in z values near one corner of B that the cap curves fail to be radially convex there. See Figure 6.

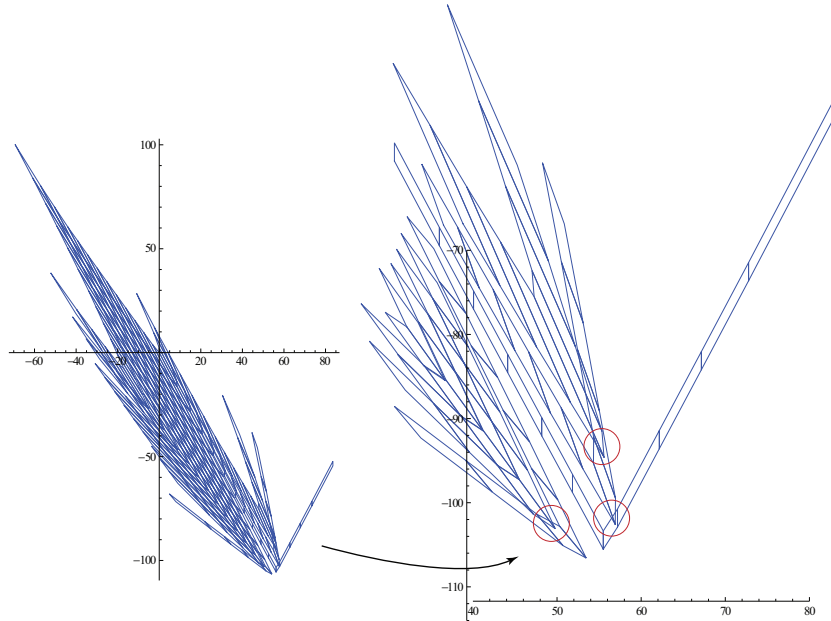


Figure 6: Overlap caused by a sharply convex cap. (Side faces are not shown.)

6 Global Non-Overlap

We have now established that all overlap is avoided locally, but there still remains the issue of possible “global overlap,” overlap of widely separated portions of the surface. It is easy to add rays to the ends of each x -strip, and rays on the sides of S_{y-} and S_{y+} , that shoot to infinity without crossing, as in Figure 7. The x -strip rays can be thought of as edges of extensions of $c_x(y)$ with long “tail” quadrilaterals extending toward $z \rightarrow -\infty$, which can be seen to preserve radial monotonicity. These rays partition the plane and separate the pieces of the unfolding from one another.

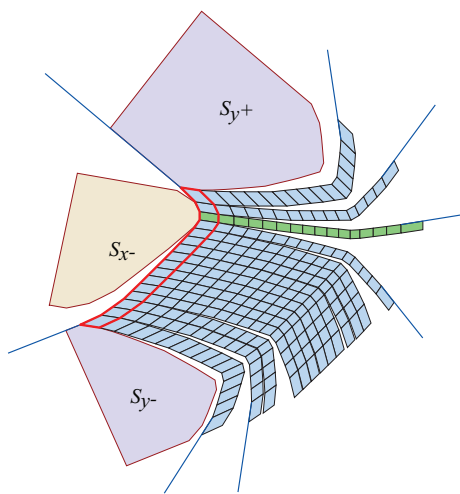


Figure 7: Extension by rays establishes global non-overlap.

7 Future Work

The class of shapes for which the presented unfolding algorithm guarantees non-overlap is narrow and of no interest except as a possible stepping stone to more general shapes. Next steps (in order of perceived difficulty) include attempting to extend the algorithm to:

1. remove the radially monotone assumption;
2. remove the assumption that B is a rectangle;
3. include shapes with both an upper and a lower convex cap surface;
4. remove the assumption that all faces are quadrilaterals.

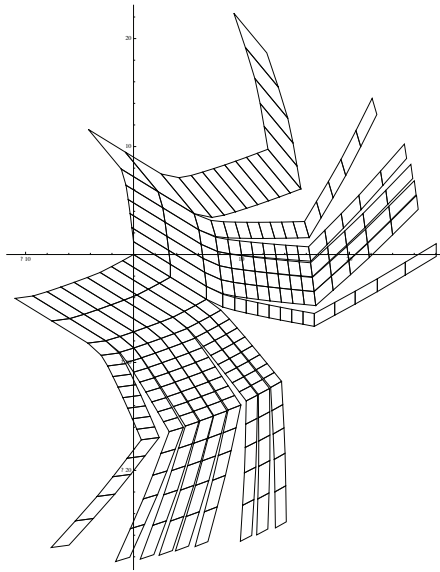


Figure 8: 16×16 cap unfolding.

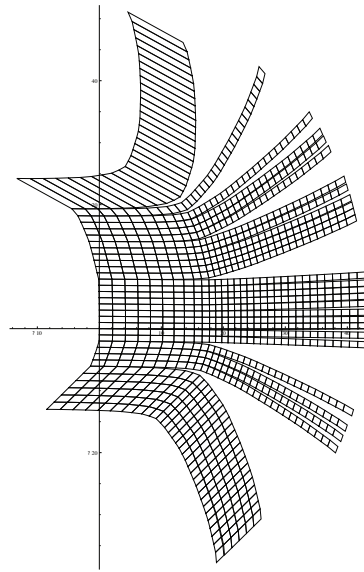


Figure 9: 32×32 cap unfolding.

References

- [DO07] Erik D. Demaine and Joseph O'Rourke. *Geometric Folding Algorithms: Linkages, Origami, Polyhedra*. Cambridge University Press, July 2007. <http://www.gfalop.org>.
- [O'R01] Joseph O'Rourke. An extension of Cauchy's arm lemma with application to curve development. In *Proc. 2000 Japan Conf. Discrete Comput. Geom.*, volume 2098 of *Lecture Notes Comput. Sci.*, pages 280–291. Springer-Verlag, 2001.
- [O'R03] Joseph O'Rourke. On the development of the intersection of a plane with a polytope. *Comput. Geom. Theory Appl.*, 24(1):3–10, 2003.